Mapping of single-site magnetic anisotropy tensors in weakly coupled spin clusters by torque magnetometry†

Luca Rigamonti,[a] Andrea Cornia,*[a] Andrea Nava,[a,b] Marie-Emmanuelle Boulon,[c,¶] Mauro Perfetti,[c] Anne-Laure Barra,[d] Xiaoliang Zhong,[e] Kyungwha Park,[e] and Roberta Sessoli[c]

[a] *Dipartimento di Scienze Chimiche e Geologiche, Università degli Studi di Modena e Reggio Emilia & INSTM RU of Modena and Reggio Emilia, via G. Campi 183, 41125 Modena, Italy. E-mail: andrea.cornia@unimore.it*

[b] *Dipartimento di Scienze Fisiche, Informatiche e Matematiche, Università degli Studi di Modena e Reggio Emilia, via G. Campi 183, 41125 Modena, Italy*.

[c] *Laboratory of Molecular Magnetism (LaMM), Dipartimento di Chimica 'Ugo Schiff', Università degli Studi di Firenze & INSTM RU of Firenze, via della Lastruccia 3-13, 50019 Sesto Fiorentino (FI), Italy.*

[d] *Laboratoire National des Champs Magnétiques Intenses, CNRS, BP166, 25 Avenue des Martyrs, 38042 Grenoble Cedex 9, France.*

[e] *Department of Physics, Virginia Tech, Blacksburg Virginia 24060, USA.*

[¶] Present address: Photon Science Institute, EPSRC School of Chemistry, The University of Manchester, Oxford Road, Manchester M13 9PL, UK.

SUPPORTING INFORMATION

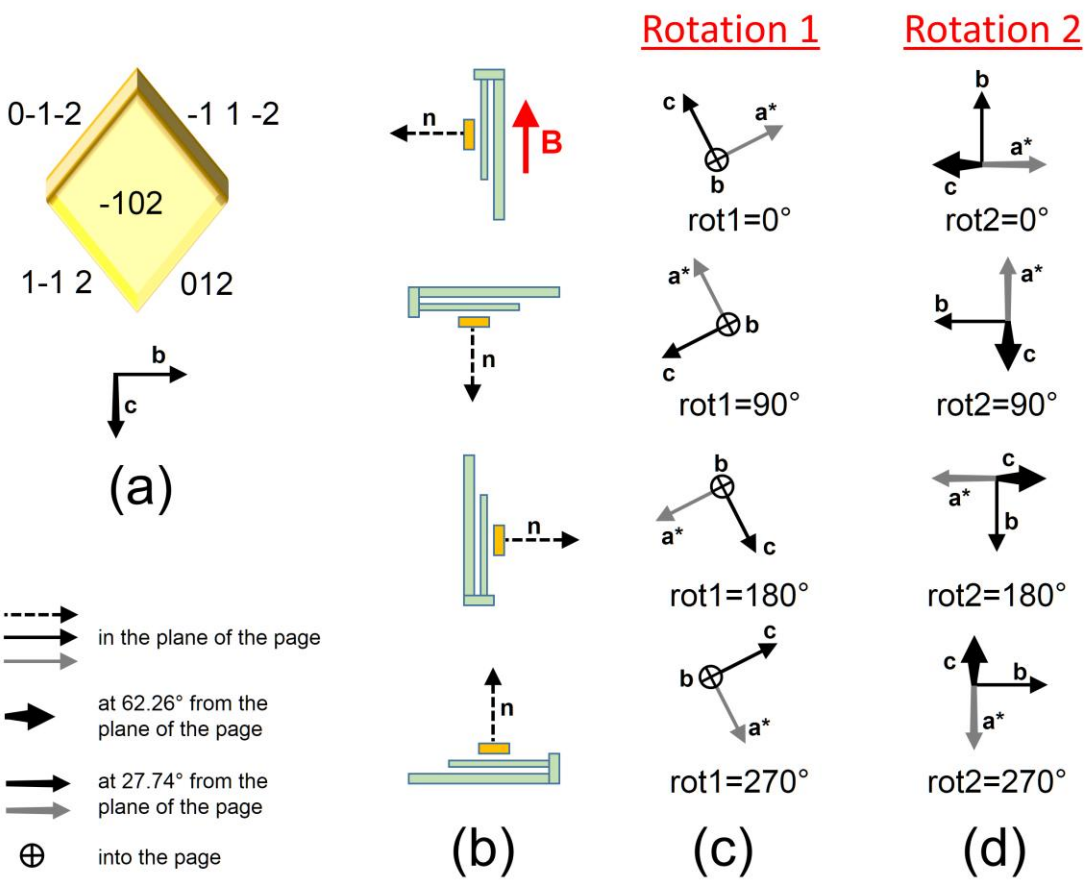

Fig. S1 Details on the geometry of torque measurements. In (a) we show face indices and the arrangement of the crystallographic axes, while in (b-d) we present the orientation of the cantilever (b) and of the crystallographic axes in the course of the two rotations for four different values of the setting angles (c, d).

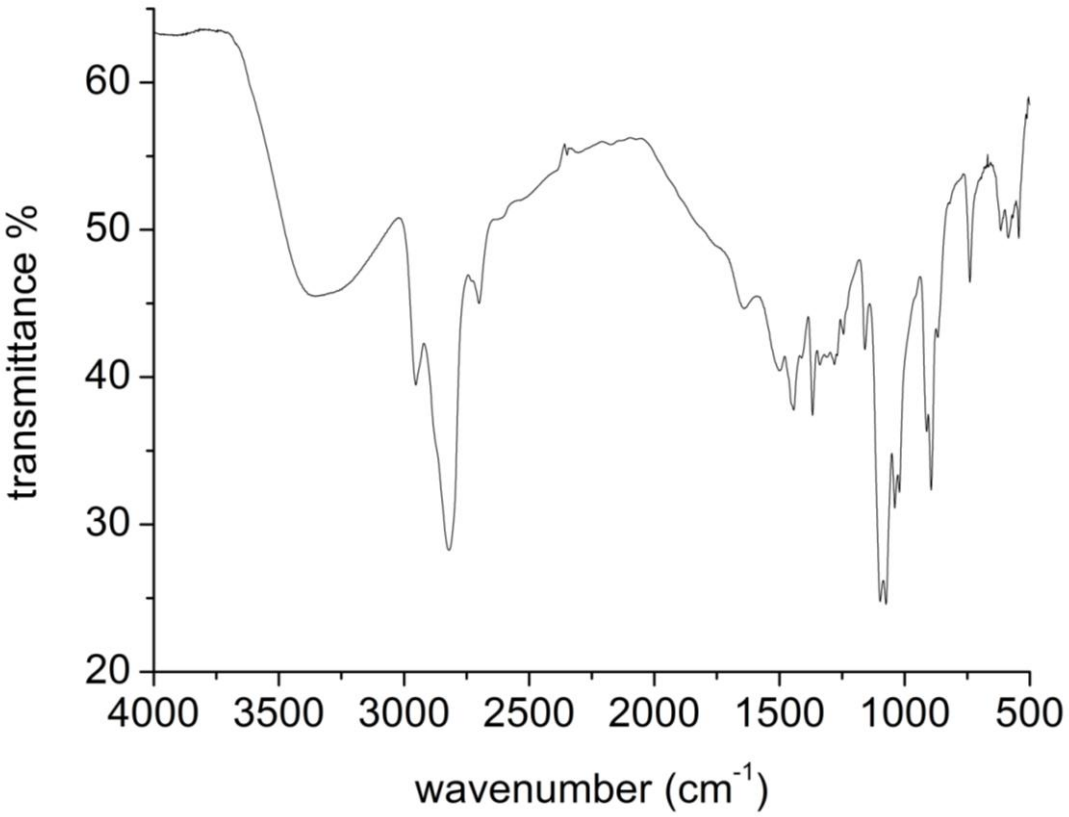
transmittance %
60
50
40
30
20
4000
3500
3000
2500
2000
1500
1000
500
wavenumber (cm-1)

(a)

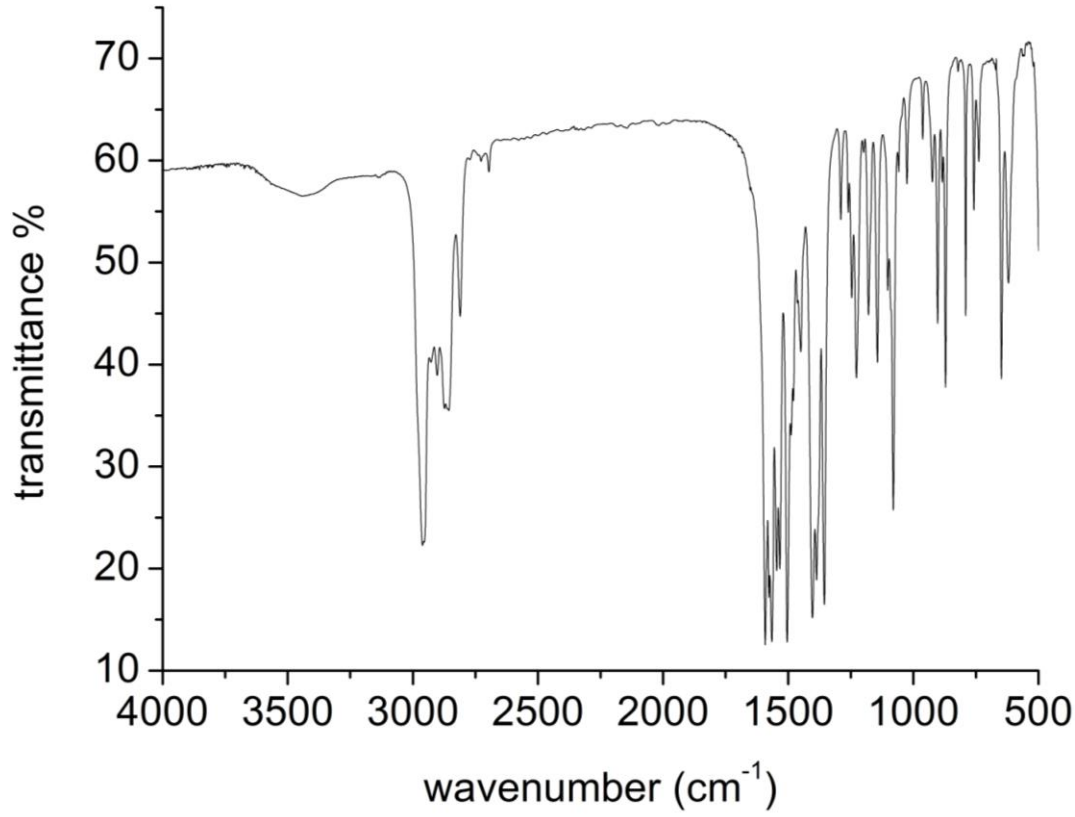
transmittance %
70
60
50
40
30
20
10
4000
3500
3000
2500
2000
1500
1000
500
wavenumber (cm-1)

(b)

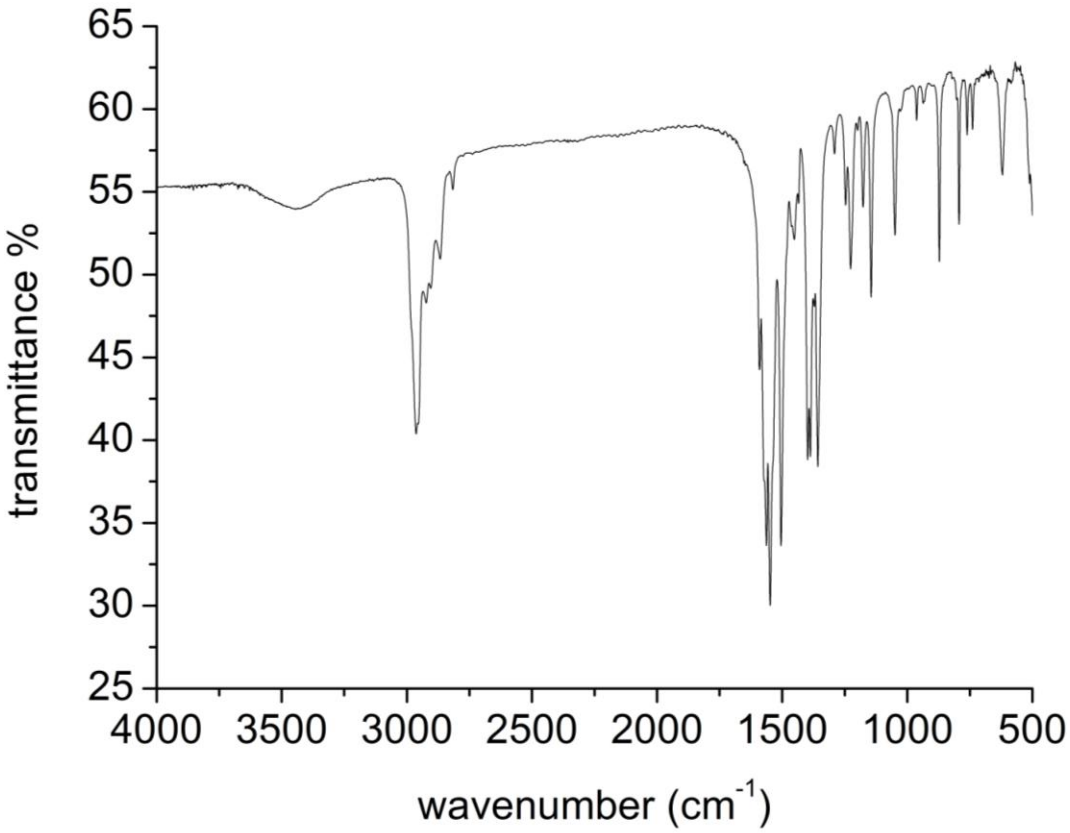

(c)

Fig. S2 Infrared spectra of $[H_3La(tea)_2]$ (a), **Fe_3La** (b), and $[Fe_2(\mu\text{-}OMe)_2(dpm)_4]$ (c) as KBr disks.

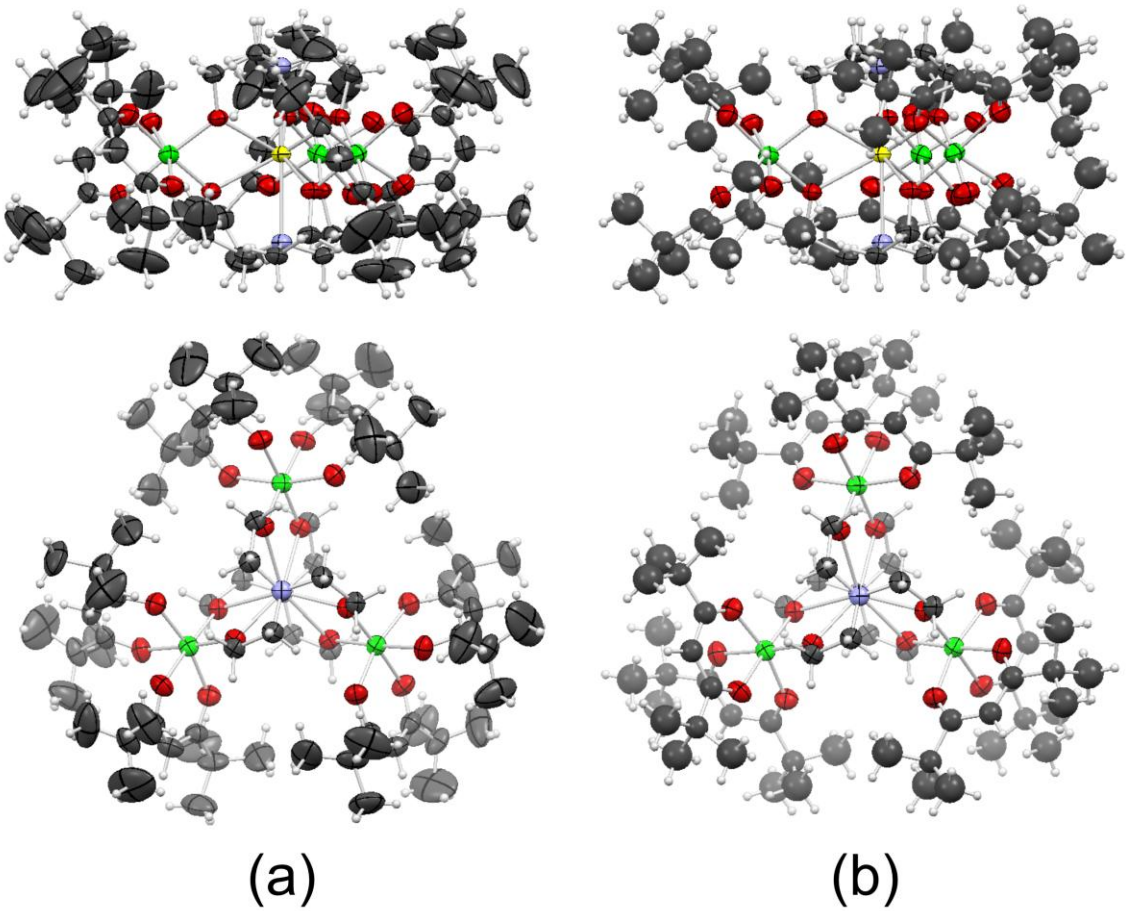

Fig. S3 Side and top views of the *ppp* (a) and *sss* (b) isomers in crystals of **Fe_3La** (La = yellow, Fe = green, O = red, N = blue, C = grey, H = white). Displacement ellipsoids are drawn at 40% probability level.

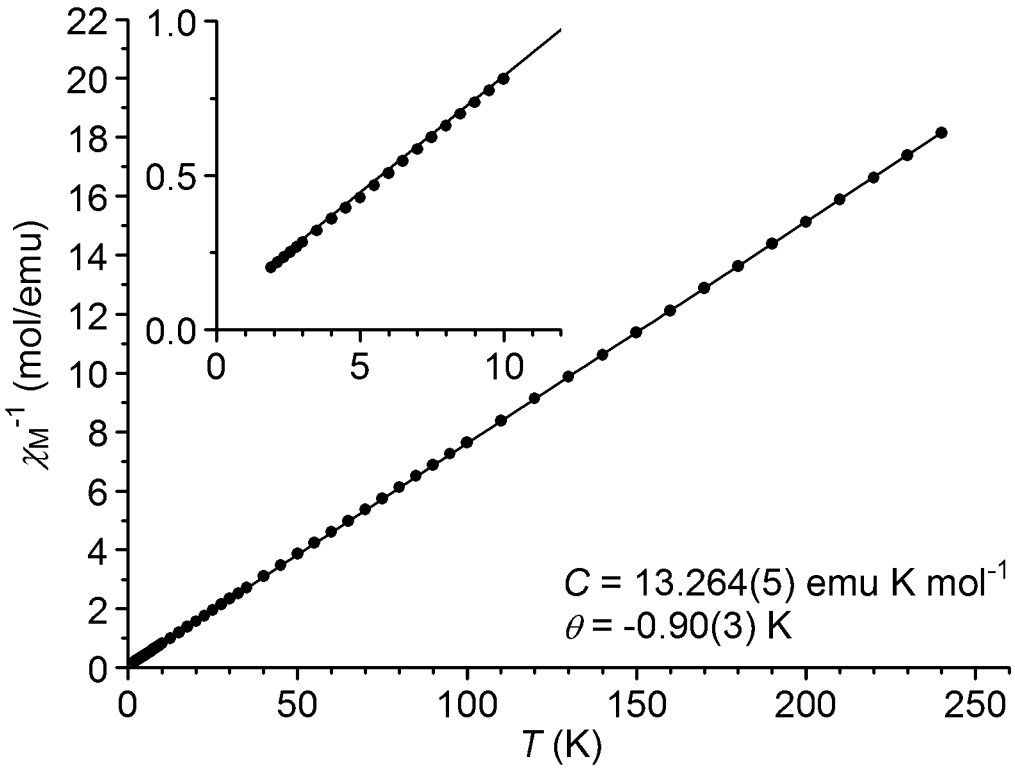

Fig. S4 Curie-Weiss plot for **Fe_3La**. The inset displays an enlargement of the low-temperature region.

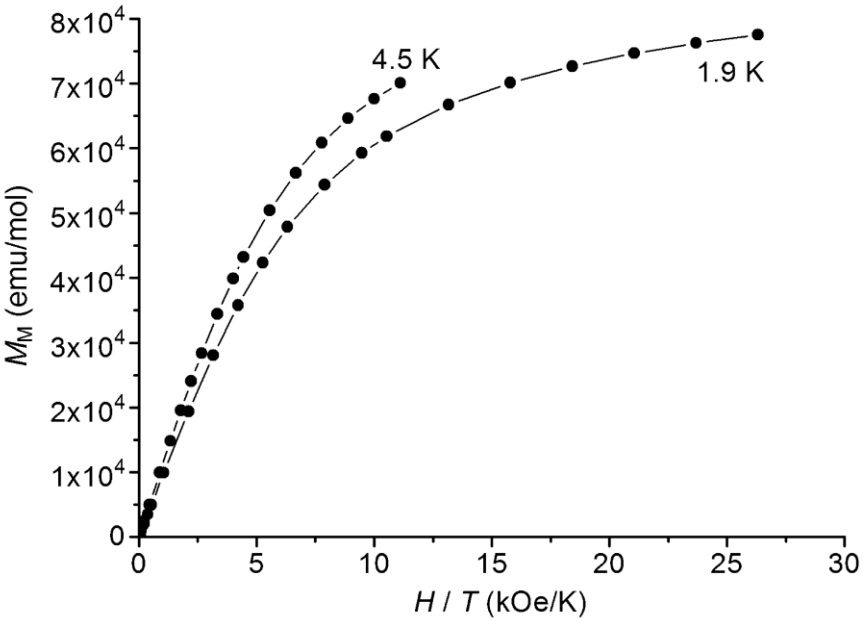

Fig. S5 Isothermal molar magnetization M_M vs. H/T data for **Fe_3La**. The nesting of curves recorded at different temperatures indicates departures from Brillouin function due to magnetic anisotropy and/or spin-spin interactions.

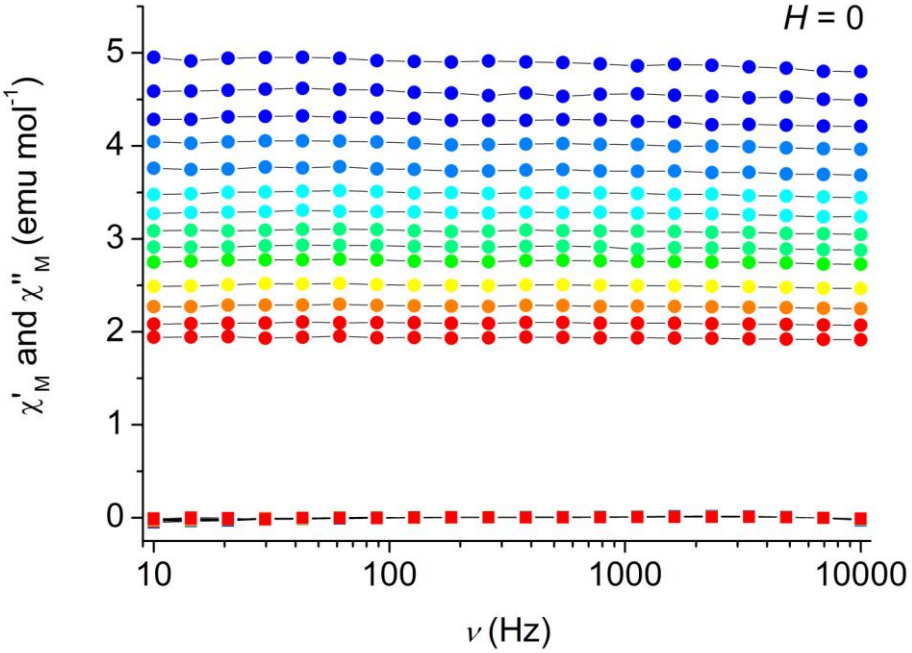

(a)

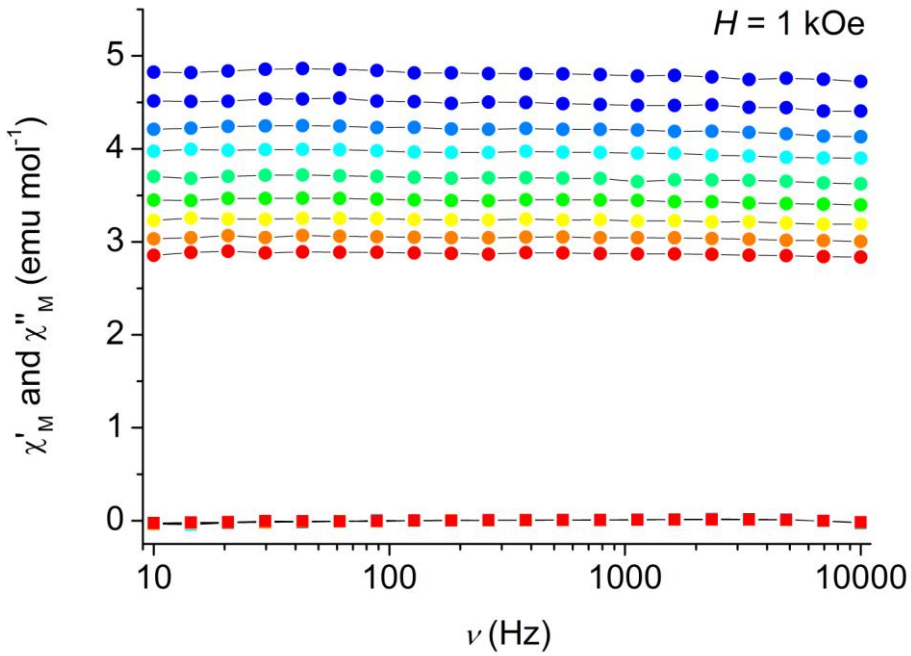

(b)

Fig. S6 Frequency dependence of the in-phase χ'_M (●) and out-of-phase χ''_M (■) AC susceptibilities of compound **Fe_3La** in zero (a) and 1-kOe (b) applied static fields and in the temperature range from 1.9 (red) to 3.5 K (blue).

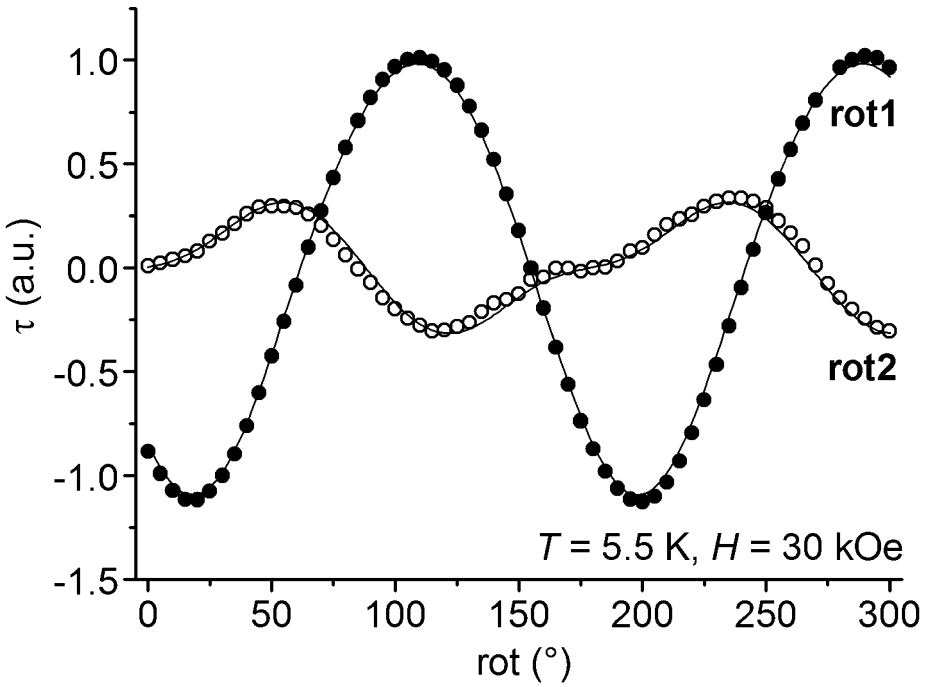

Figure S7. Torque signal for **rot1** and **rot2** at 5.5 K and 30 kOe. The cantilever was sensitive to the torque component along the green and blue arrows, respectively, in Fig. 3. The solid curves were calculated with the spin-Hamiltonian parameters, scale factors and angular offsets that provide the best fit to the 2.3 K data in Figs. 4 and 5.

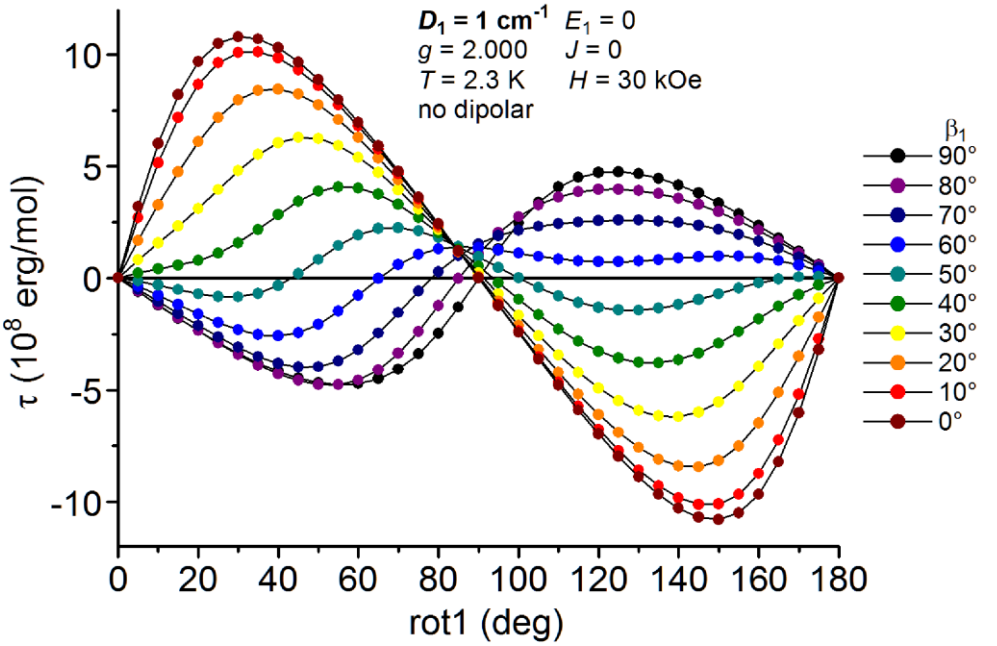
D_1 = 1 cm^{-1} E_1 = 0
g = 2.000 J = 0
T = 2.3 K H = 30 kOe
no dipolar
τ (10^8 erg/mol)
rot1 (deg)
β1
90°
80°
70°
60°
50°
40°
30°
20°
10°
0°

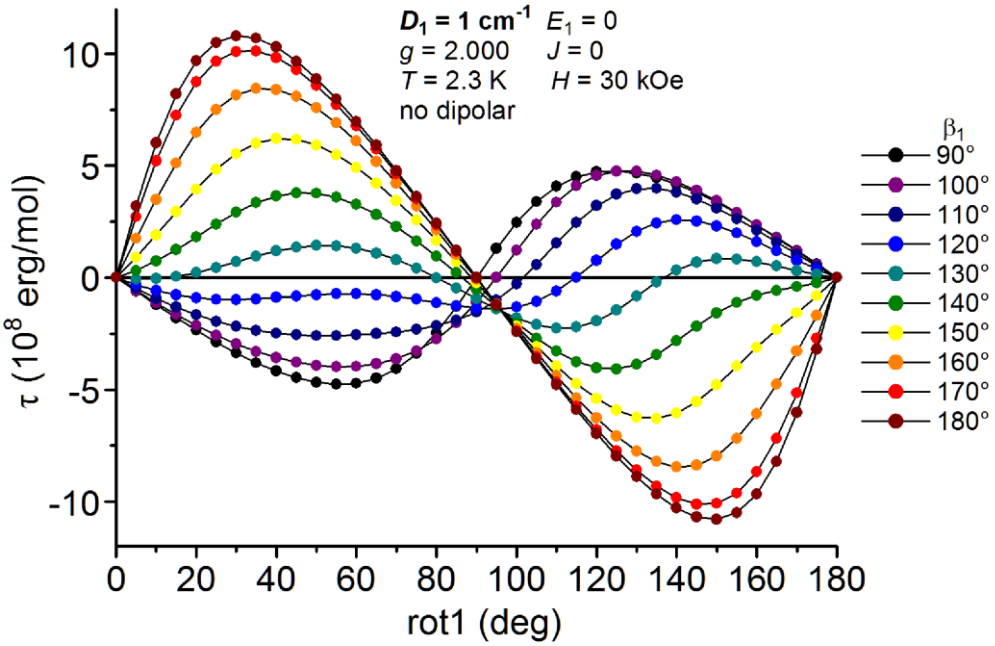
D_1 = 1 cm^{-1} E_1 = 0
g = 2.000 J = 0
T = 2.3 K H = 30 kOe
no dipolar
τ (10^8 erg/mol)
rot1 (deg)
β1
90°
100°
110°
120°
130°
140°
150°
160°
170°
180°

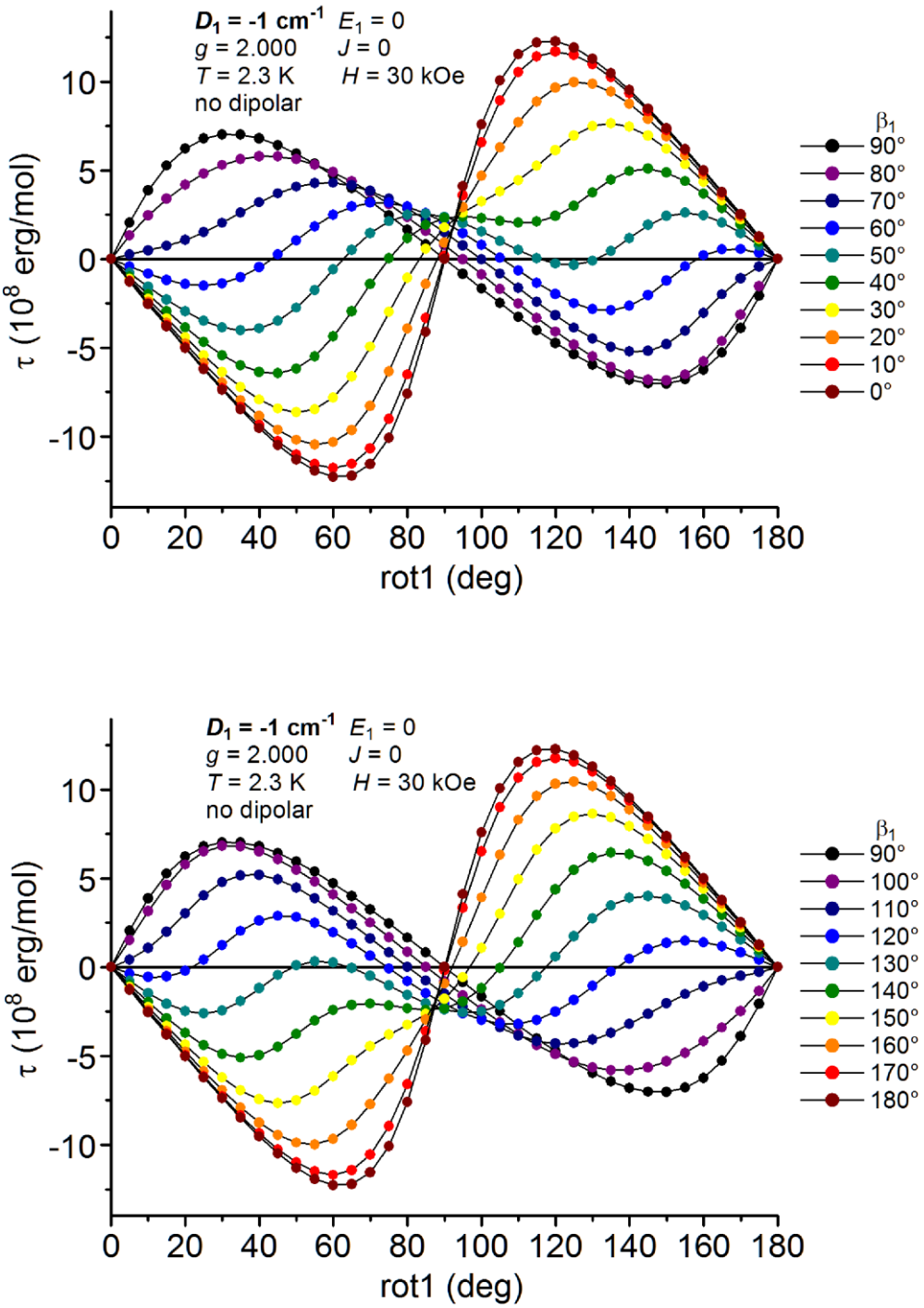

Fig. S8 Torque signal for **rot1** calculated with the indicated set of spin Hamiltonian parameters and for different values of the Euler angle β_1. Here, an offset of +27.74° was added to the rotation angle as defined in Fig. 3, so that at rot1 = 0 the magnetic field is directed along the **c** axis. The reported component of the torque is that along the green arrow in Fig. 3. Notice that curves are antisymmetric with respect to rot1 = 0 (mod 90) only for β_1 = 0, 90° and 180°.

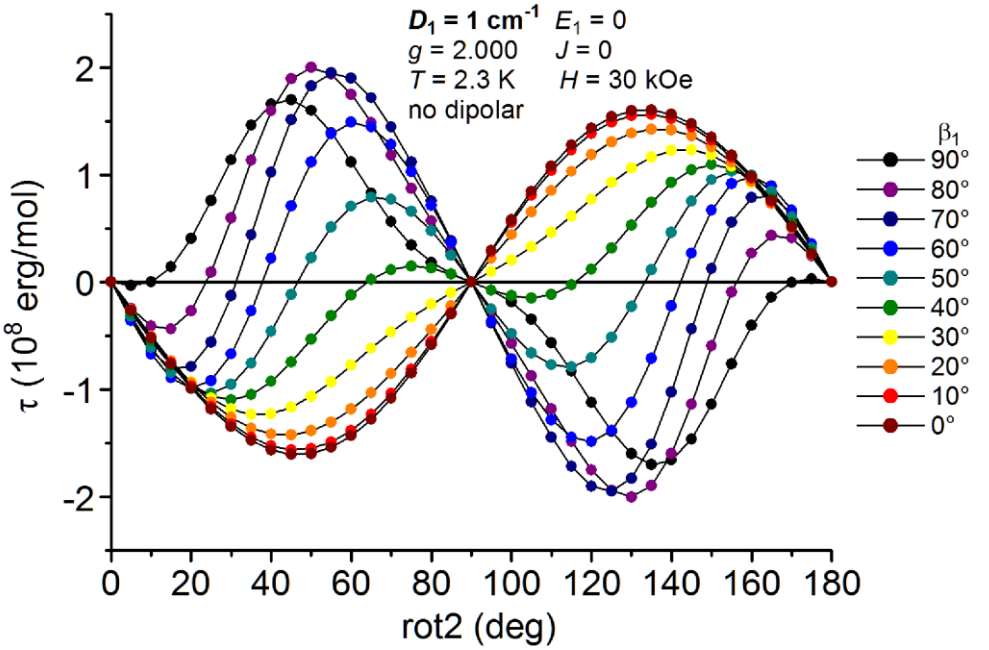
D_1 = 1 cm^{-1} E_1 = 0
g = 2.000 J = 0
T = 2.3 K H = 30 kOe
no dipolar
τ (10^8 erg/mol)
rot2 (deg)
β1
90°
80°
70°
60°
50°
40°
30°
20°
10°
0°

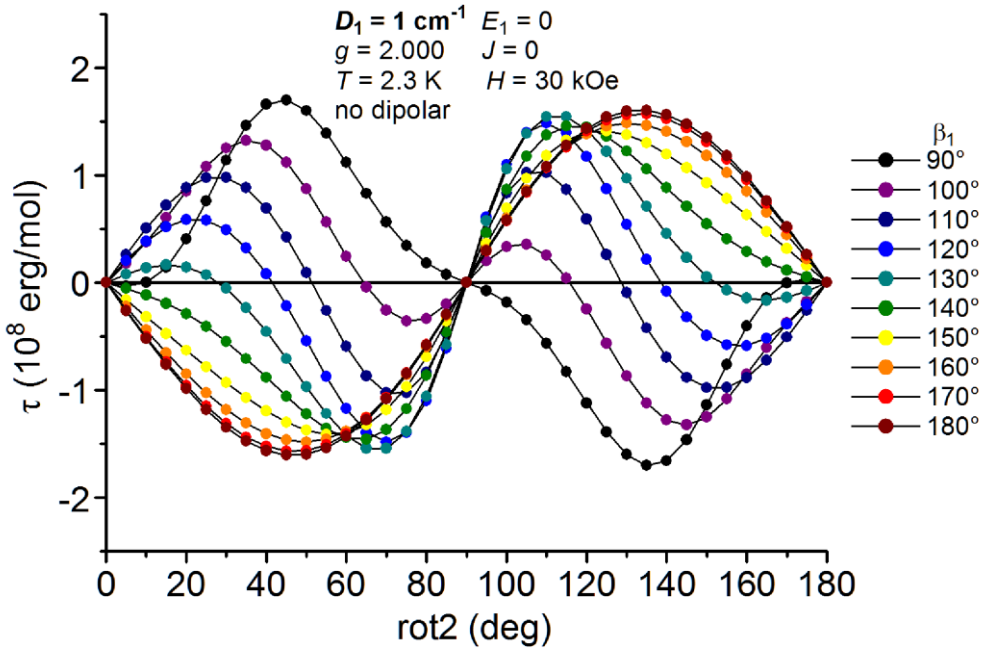
D_1 = 1 cm^{-1} E_1 = 0
g = 2.000 J = 0
T = 2.3 K H = 30 kOe
no dipolar
τ (10^8 erg/mol)
rot2 (deg)
β1
90°
100°
110°
120°
130°
140°
150°
160°
170°
180°

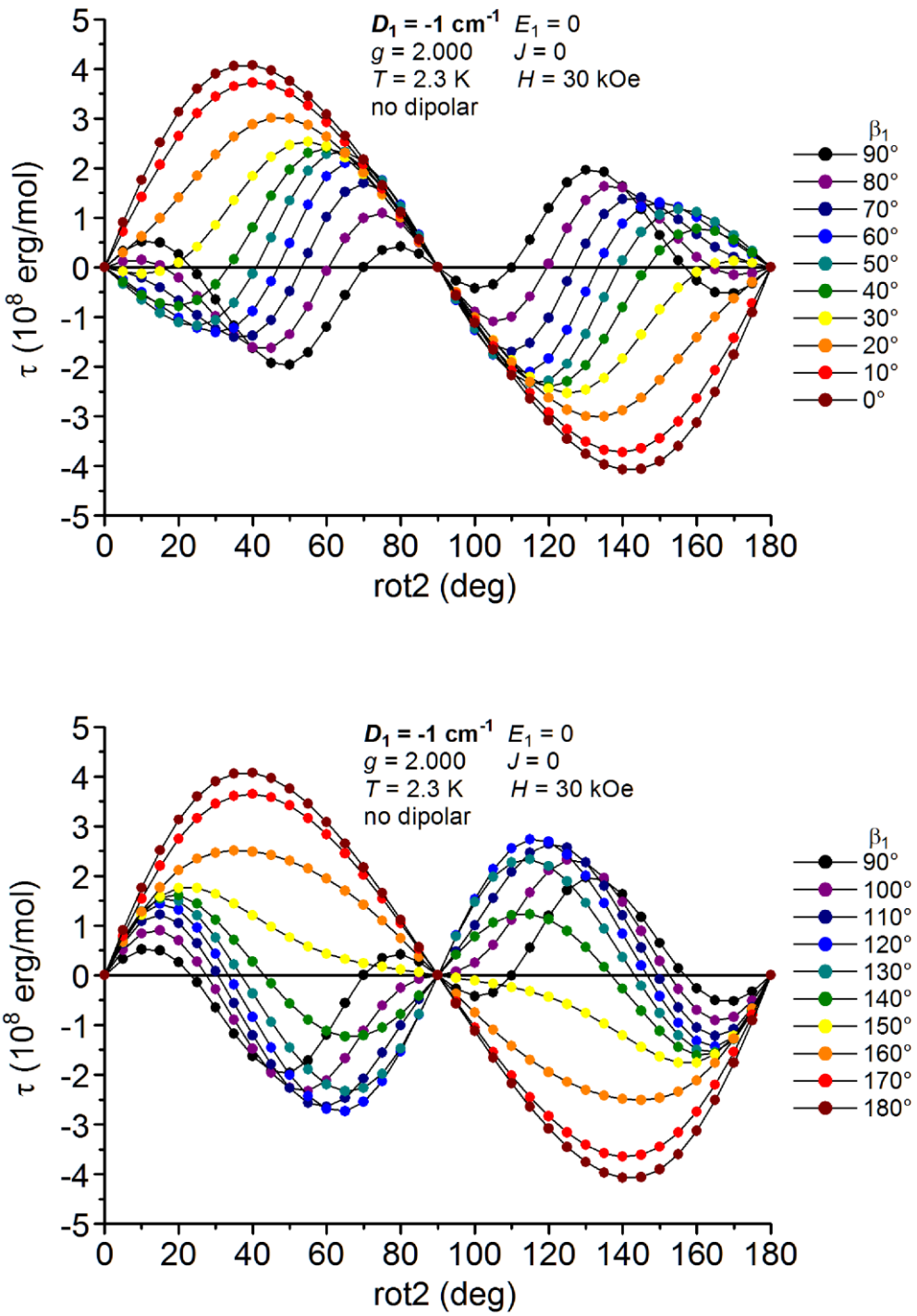

Fig. S9 Torque signal for **rot2** calculated with the indicated set of spin Hamiltonian parameters and for different values of the Euler angle β_1. Here, the rotation angle is the same as defined in Fig. 3, so that at rot2 = 0 the magnetic field is directed along the **b** axis. The reported component of the torque is that along the blue arrow in Fig. 3. Notice that all curves are antisymmetric with respect to rot2 = 0 (mod 90).

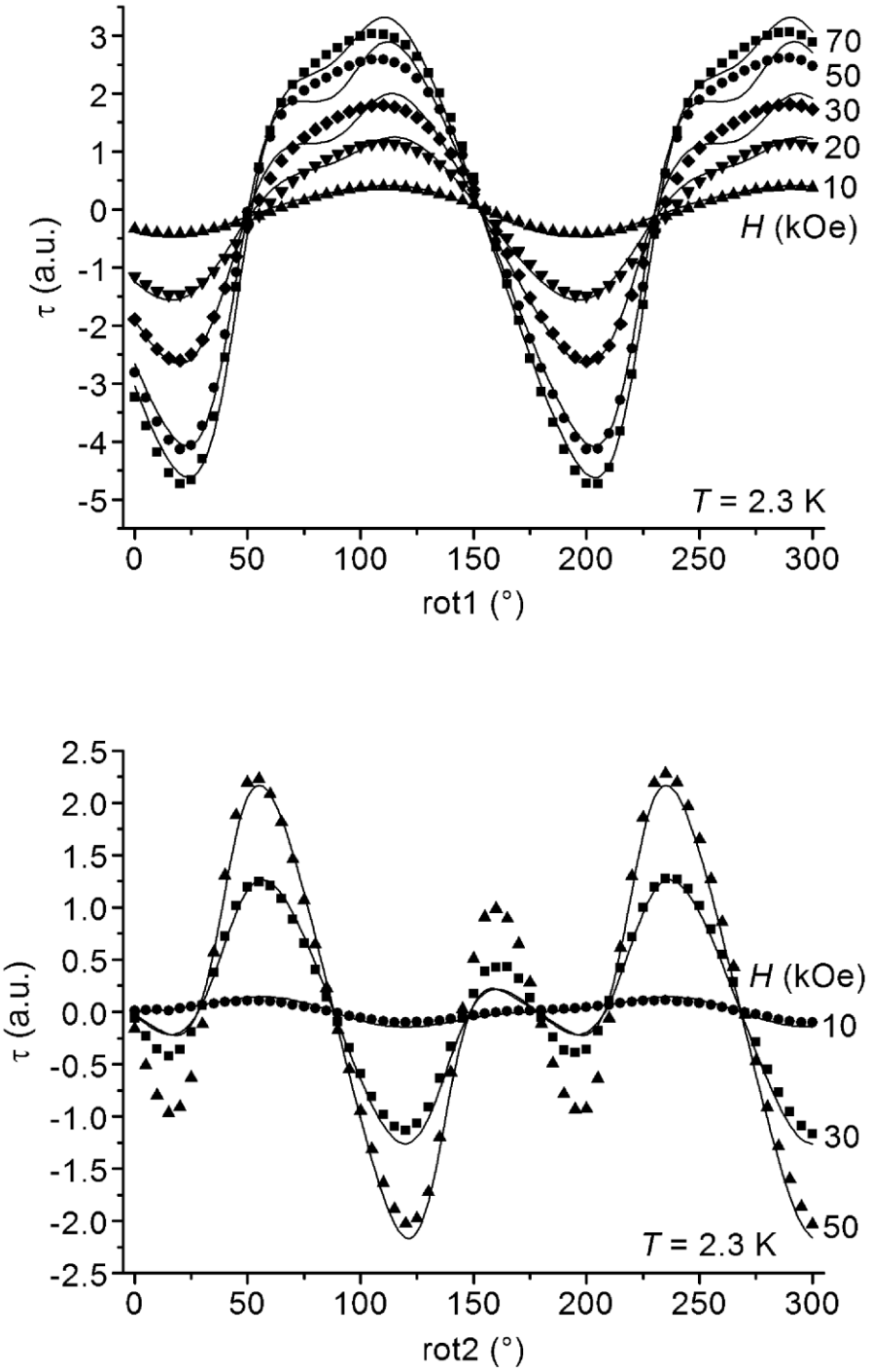

Fig. S10 Best-fit simulation of torque data at 2.3 K with $D_1 < 0$ (D_1 = –1.34(3) cm^{-1}, E_1 = –0.320(18) cm^{-1}, J = 0.066(7) cm^{-1}, β_1 = 35.1(4)°, k_1 = 0.304(7), k_2 = 0.368(10), θ_1 = –0.61(19)°, θ_2 = 1.8(3)°, $\chi^2 = 2.87 \times 10^{-2}$).

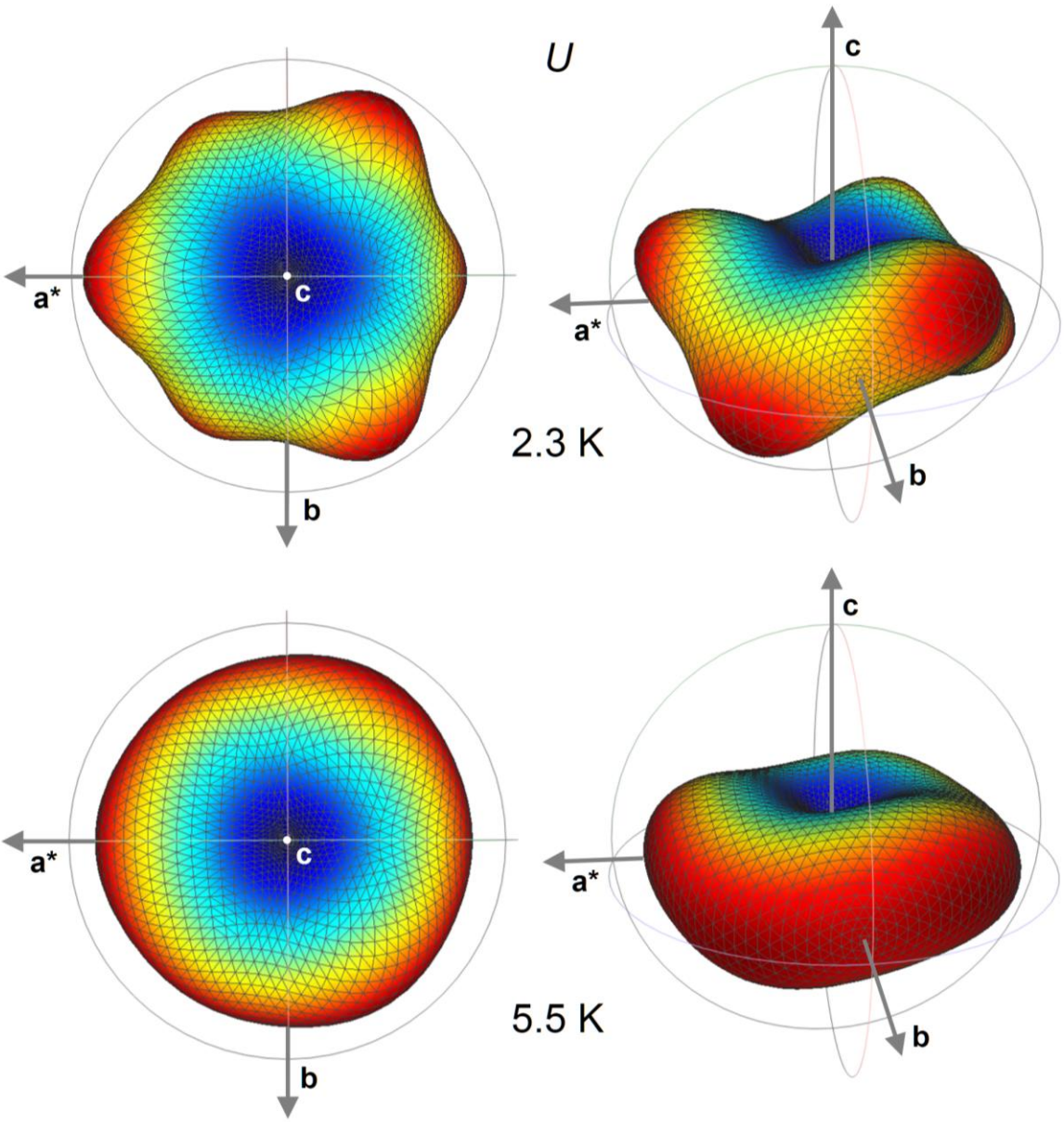

Fig. S11 Internal energy surfaces of **Fe_3La** computed with the set of best-fit spin Hamiltonian parameters for different orientations of a 30-kOe magnetic field at 2.3 and 5.5 K. The distance from the centre of the diagram is proportional to $U - U_{min}$, where U_{min} is the minimum value of the internal energy that is found when the field is applied along **c**. The angular dependence of U is also displayed using a colour scale (from blue to red).

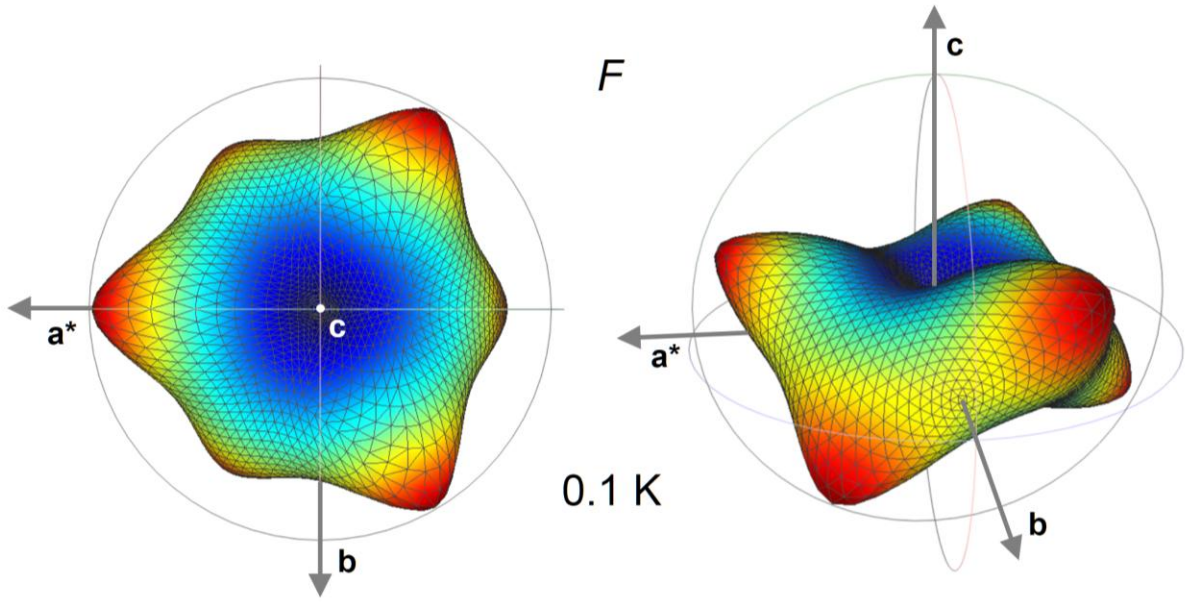

Fig. S12 Free energy surface of **Fe_3La** computed with the set of best-fit spin Hamiltonian parameters for different orientations of a 30-kOe magnetic field at 0.1 K. The distance from the centre of the diagram is proportional to $F - F_{min}$, where F_{min} is the minimum value of the free energy that is found when the field is applied along **c**. The angular dependence of F is also displayed using a colour scale (from blue to red).

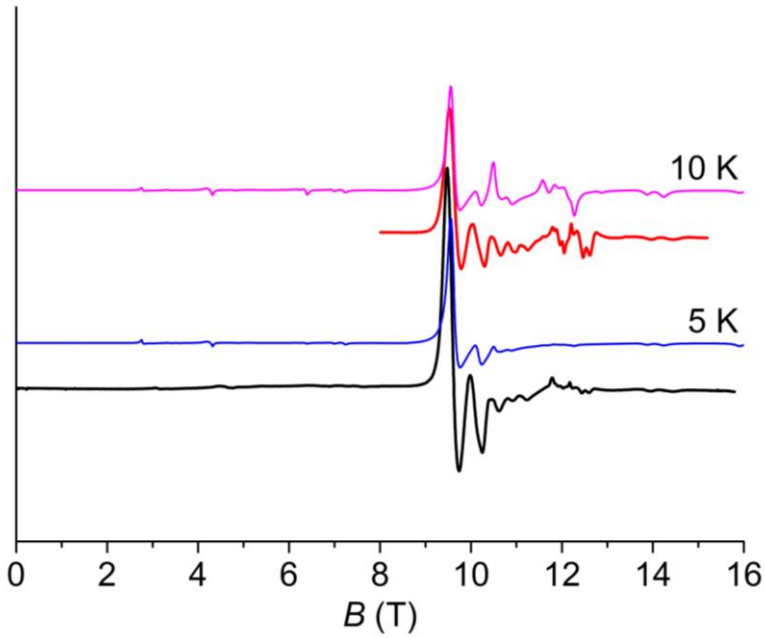

Fig. S13 EPR powder spectra (331.2 GHz) of **Fe_3La** at 5 and 10 K. Experimental spectra are drawn in black and red, while blue and pink curves are calculated spectra for independent (J = 0) iron(III) sites with D_1 = 0.95 cm^{-1}, E_1 = 0.04 cm^{-1}, $D_2 = D_3$ = 1.12 cm^{-1}, $E_2 = E_3$ = 0, ΔD_1 = 0.02 cm^{-1}, $\Delta D_2 = \Delta D_3$ = 0.04 cm^{-1} and an isotropic g = 2.00 in all cases.

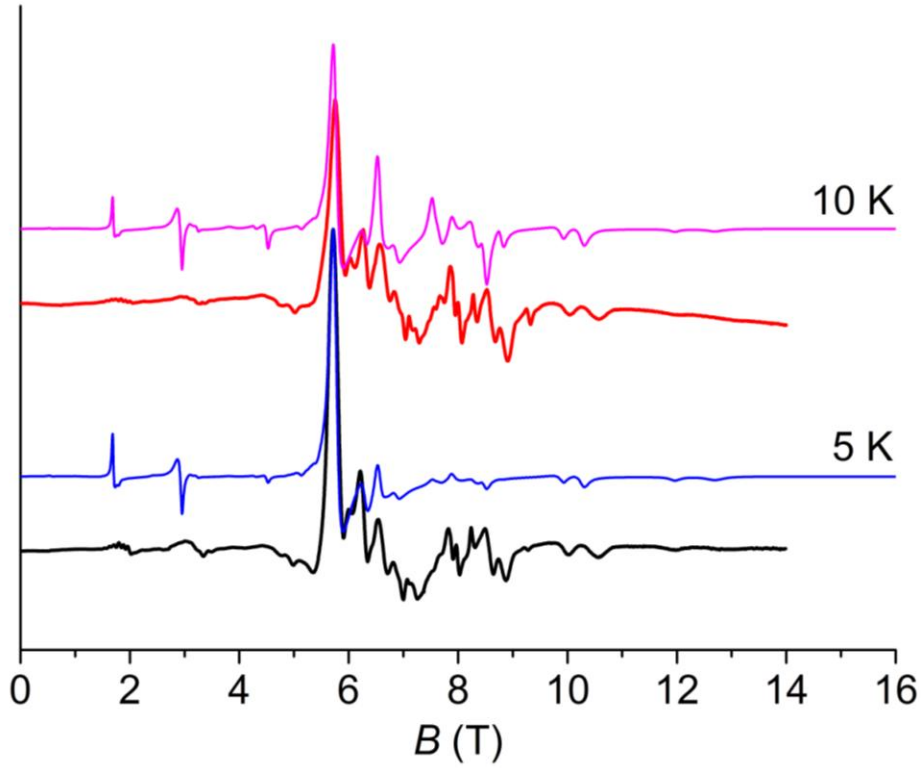

Fig. S14 EPR powder spectra (220.8 GHz) of **Fe_3La** at 5 and 10 K. Experimental spectra are drawn in black and red, while blue and pink curves are calculated spectra for independent (J = 0) iron(III) sites with D_1 = 0.95 cm^{-1}, E_1 = 0.04 cm^{-1}, $D_2 = D_3$ = 1.12 cm^{-1}, $E_2 = E_3$ = 0, ΔD_1 = 0.02 cm^{-1}, $\Delta D_2 = \Delta D_3$ = 0.04 cm^{-1} and an isotropic g = 2.00 in all cases.

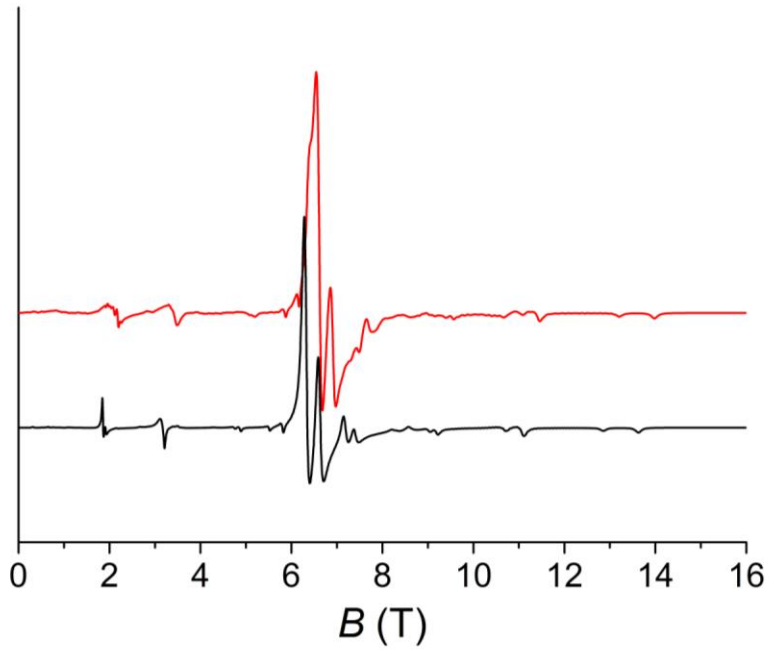

(a)

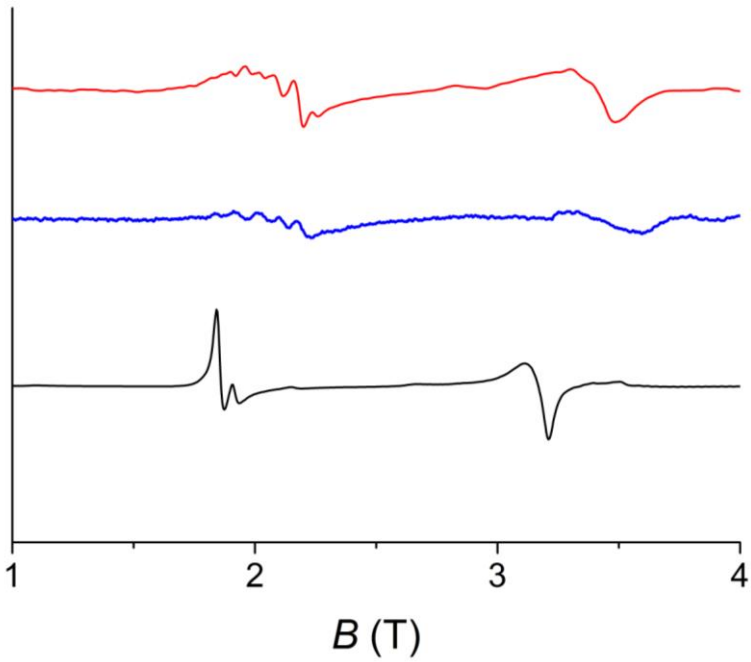

(b)

Fig. S15 (a) Calculated EPR powder spectra at 240.0 GHz and 5 K with D_1 = 1.00 cm^{-1}, D_2 = D_3 = 1.18 cm^{-1}, E_1 = E_2 = E_3 = 0, β_1 = β_2 = β_3 = 90° and an isotropic g = 2.00. The black and red curves correspond to J = 0 and J = 0.064 cm^{-1}, respectively. (b) Zoom over the forbidden transitions together with the experimental spectrum of **Fe$_3$La** (blue curve).

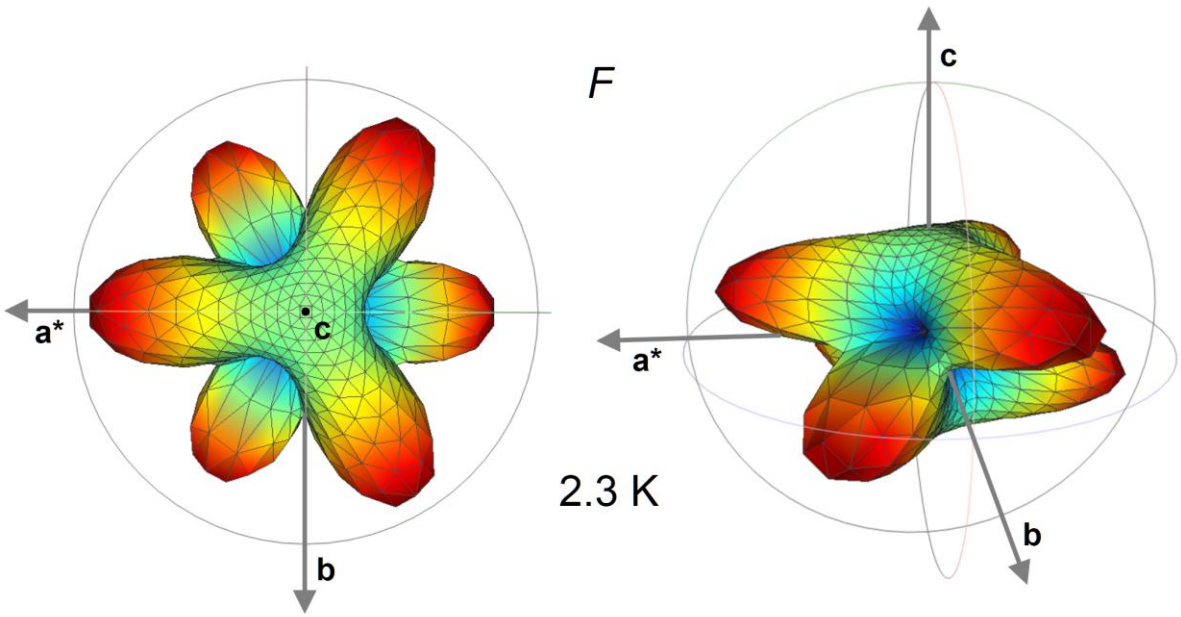

Fig. S16 Free energy surface of **Fe_4** computed using van Wüllen single-ion parameters for different orientations of a 30-kOe magnetic field at 2.3 K. The axial components $B_2^0\hat{O}_2^0$, $B_4^0\hat{O}_4^0$ and $B_6^0\hat{O}_6^0$ have been subtracted from the data to better display the high-order modulations arising from $B_4^3\hat{O}_4^3$, $B_6^3\hat{O}_6^3$ and $B_6^6\hat{O}_6^6$. The distance from the centre of the diagram is proportional to $F - F_{min}$, where F_{min} is the minimum value of the free energy that is found when the field is applied along **c**. The angular dependence of F is also displayed using a colour scale (from blue to red). The best-fit set of parameters required to reproduce the pristine free energy surface is: $D(5) = 3B_2^0 = -0.433$ cm^{-1}, $B_4^0 = 1.51 \times 10^{-5}$ cm^{-1}, $B_4^3 = 8.95 \times 10^{-5}$ cm^{-1}, $B_6^0 = 1.74 \times 10^{-8}$ cm^{-1}, $B_6^3 = -1.10 \times 10^{-7}$ cm^{-1} and $B_6^6 = 6.09 \times 10^{-8}$ cm^{-1}.